



Semnan University

# Applied Chemistry Today

Journal homepage: <https://chemistry.semnan.ac.ir/>

ISSN: 2981-2437

*Research Article*

## Synthesis and Characterization of a Novel Nonionic Glucosamine-Based Surfactant and its Comparison with *N*-Methylglucamine Surfactant

Syedeh Enciyeh Rastegar Fatemi<sup>a</sup>, Hadi Shafiei<sup>a,\*</sup> , Mohammad Majid Mojtahedi<sup>b</sup> <sup>a</sup>Department of Chemistry, Arak Branch, Islamic Azad University, Arak, Iran<sup>b</sup>Organic Chemistry Department, Chemistry and Chemical Engineering Research Center of Iran, P.O. Box 14335-186, Tehran, Iran**PAPER INFO****Article history:**

Received: 09/Apr/2024

Revised: 29/Jun/2024

Accepted: 30/Jun/2024

**Keywords:**Non-ionic surfactant,  
Surface tension,  
Glucosamine,  
Emulsifier,  
Hydrophilicity-  
lipophilicity balance.**ABSTRACT**

In this study, the synthesis, surface evaluation, and thermodynamics properties a novel non-ionic glucosamine-based surfactant (2-(dodecyloxy)-*N*-((2*R*,3*R*,4*R*,5*S*,6*R*)-2,4,5-trihydroxy-6-(hydroxymethyl)tetrahydro-2*H*-pyran-3-yl)acetamide (NGAS) is carried out and the comparison of the results with *N*-methylglucamine surfactant is reported. NGAS was synthesized via the facile and straightforward reaction of glucosamine with 2-(dodecyloxy) acetyl chloride in the presence of triethylamine. The surface tension of NGAS was determined by tensiometric methods. The surface properties including Critical Micelle Concentration (CMC), the efficiency of adsorption (pC<sub>20</sub>), the surface excess (Γ<sub>max</sub>) and the area occupied by each of the surfactant molecules (A<sub>min</sub>) were investigated at 298.15 K in deionized water. The surface tension of water was reduced to about 41 mN.m<sup>-1</sup> by using the surfactant at the concentration level of 2.06×10<sup>-3</sup> molL<sup>-1</sup>. The thermodynamic parameters of micellization (ΔG<sup>o</sup><sub>mic</sub>) and surface adsorption (ΔG<sup>o</sup><sub>ads</sub>) were calculated from CMC data. The hydrophilicity and lipophilicity balance parameter (HLB) were obtained from the Griffin equation. According to the results, micellization and surface adsorption of this surfactant is a spontaneous process in aqueous solution. In addition, these results show that NGAS can be used as an emulsifier in oil-in-water emulsions.

DOI: <https://doi.org/10.22075/chem.2024.33744.2265>

© 2024 Semnan University.

This is an open access article under the CC-BY-SA 4.0 license. (<https://creativecommons.org/licenses/by-sa/4.0/>)

\*corresponding author: Assistant Professor of Physical Chemistry. Email address: hshafie2005@yahoo.com

**How to cite this article:** Rastegar Fatemi, S. E., Shafiei, H., & Mojtahedi, M. M. (2024). Synthesis and Characterization of a Novel Nonionic Glucosamine-Based Surfactant and its Comparison with *N*-Methylglucamine Surfactant. *Applied Chemistry Today*, **19(73)**, 91-102. (in Persian)

## 1. Introduction

Surfactants are considered as essential materials in numerous industries, including personal care formulations and cleaning products, since they are able to reduce the surface tension between different phases [1, 2]. The four main types of surfactants are categorized in anionic, cationic, non-ionic, and amphoteric [3-8] subgroups. Among these categories, non-ionic surfactants are widely used in personal care formulations, due to their compatibility with various ionic strengths and pH levels. Recently, non-ionic sugar-based surfactants have gained significant attention, owing to their unique properties, including remarkable mildness, biodegradability, and excellent cleaning ability [9-12]. Moreover, they exhibit low toxicity and are gentle on sensitive skins, being ideal for personal care products such as body washes, hand soaps, facial cleaners, and shampoos [13-18]. Based on these features, non-ionic sugar-based surfactants are considered as a sustainable alternative to traditional surfactants. In this context, glucosamine-based surfactants have especially gained popularity, due to their superior surface activity, low toxicity, and emulsification properties, making them suitable for various applications in the industry [19-29]. Comprehensive evaluation and discussion in this context are presented in three recent reviews, compiling and describing related useful synthetic methods for the production of sugar-based surfactants [30-32].

In this study, the synthesis and evaluation of a sugar-based surfactant derived from glucosamine was carried out for the first time in both computational and experimental levels. In the computational phase, all geometrical optimizations and energy calculations were performed using the M06-2X function and the 6-31 G (d, p)-basis, being set on the structure of the new sugar-based surfactant derived from glucosamine (NGAS). The results showed that NGAS has high solvation energy and excellent solubility in water [33], and is synthesized based on this procedure. Next, we conducted the experimental phase by evaluating the properties and structure of NGAS. Characterization of NGAS was performed using FTIR and mass analyses. In addition, the critical micelle concentration (CMC) value was obtained using surface tension measurement at 298.15 K. The parameters affecting the micellization and interfacial behaviors such as  $\Gamma_{\max}$  (maximum surface excess concentration), CMC, the surface tension at the CMC ( $\gamma_{\text{CMC}}$ ), free energies of micellization ( $\Delta G^{\circ}_{\text{m}}$ ), and free energies of adsorption ( $\Delta G^{\circ}_{\text{ads}}$ ) were also surveyed. Due to similarity of the chemical structure of NGAS and the non-ionic surfactant *N*-methylglucosamine (C12GA), the surface properties of the two surfactants were compared. Both surfactants differ in the type and the size of their hydrophilic head groups, but have exactly the same side alkyl chain (12 carbon atoms tail). Structures of the two surfactants are shown in Fig. 1.

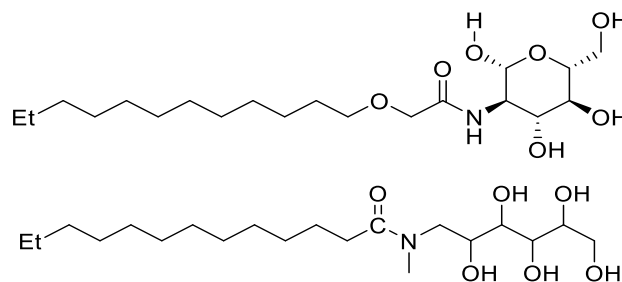


Fig. 1. NGAS (top) and C12GA (bottom) with 12-carbon aliphatic chain

## 1. Experimental

### 2.1. Materials and instrumentation

1-Dodecanol ( $\geq 98.0\%$ ), sodium chloroacetate (98%), thionyl chloride (97%), and glucosamine

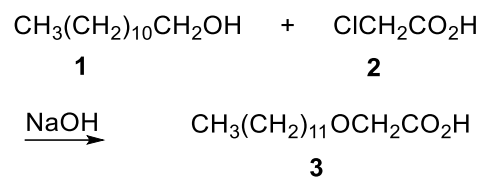
hydrochloride ( $\geq 99\%$ ) were purchased from Sigma-Aldrich Company and used as received. Triethylamine ( $\geq 99.5\%$ ), sodium hydroxide ( $\geq 97.0\%$ ), hydrochloric acid ( $37\%$ ) were purchased from Merck Company and used as received. Fourier Transform Infrared (FT-IR) spectra were recorded on an ABB Bomem MB-100 spectrometer, using KBr pellet for sample preparation. Mass spectra were carried out on an Agilent 5975C instrument at 70 eV. The surface tensions of the surfactant were measured at 298.15 K, using a Krüss K12 tensiometer and du Nouy ring, calibrated with deionized water and thermostated to within  $\pm 0.05$  °C. All glassware were rinsed with acetone and then with double distilled water, prior to be used. Prior to each measurement, the platinum ring was cleaned by using acetone followed by rinsing with double-distilled water and then it being heated briefly by being held above a Bunsen burner until glowing. The value of the critical micelle concentration was obtained from the intersection of the two lines in low and high concentrations areas of the surface tension curves. Surfactant solutions were prepared with double-distilled water. A stock solution (2000 ppm) was prepared in double-distilled water and it was used for the preparation of more dilute solutions (10-1500 ppm). The surface tension of the deionized water was measured prior to the measurement of the stock solutions, starting from the most dilute solution. This value was  $72.1 \pm 0.2$  mNm<sup>-1</sup>. All reported experimental values are the average of three measurements.

## 2.2. Synthesis of NGAS

The synthesis of the glucosamine-based surfactants involves three steps, including the preparation of the required fatty acid from the corresponding fatty alcohol, conversion of the fatty acid to the corresponding fatty acyl chloride, and synthesis of the glucosamine-based surfactant, NGAS. For the first two steps, a known procedure was used [34,

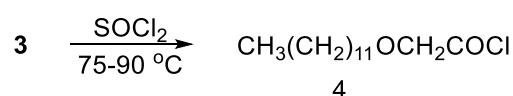
35]. Detailed procedures for each step are provided in the following.

### 2.2.1. Preparation of 2-dodecoxyacetic acid from 1-dodecanol



In order to synthesize 2-dodecoxyacetic acid, a reaction was carried out using 1-dodecanol (9.3 g, 50 mmol) in a 250 mL round bottom flask. The reaction was conducted at 70 °C with the aid of a magnetic heater stirrer. To the flask, were added NaOH (2.2 g, 55 mmol) and sodium monochloroacetate (6.4 g, 55 mmol) and the mixture was continued to stir for another 5 hours at 70 °C. The completion of the reaction was monitored by thin layer chromatography (TLC), using ethyl acetate/petroleum ether (4:1) as the eluent. The resulting precipitate was filtered by a Buchner funnel and washed with 10 mL of 32% HCl. The alkyl ether carboxylic acid (2-dodecoxyacetic acid) was obtained as the product 3 (10.9 g, 90%).

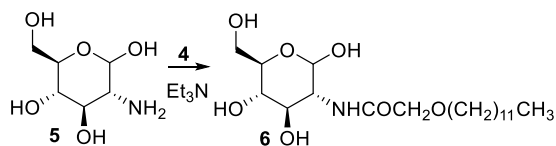
### 2.2.2. Conversion of 2-dodecoxyacetic acid to fatty acyl ether chloride



For the synthesis of the fatty acyl chloride, a 250 mL three-necked flask was equipped with a dropping funnel, a reflux condenser, a mechanical stirrer, and a thermometer. 2-Dodecoxyacetic acid 3 (4.88 g, 20 mmol) was introduced to the flask, followed by gradual addition of thionyl chloride (3 mL, 40 mmol) within 2.5 hours, maintaining vigorous stirring throughout the mixing. Then, the reaction mixture was heated at 90 °C for 4 hours. The completion of the reaction was monitored by TLC, using ethyl acetate/petroleum ether (4:1) as the eluent. The excess thionyl chloride was removed

under vacuum. The fatty acyl ether chloride 4 was obtained in 85% yield (4.5 g).

### 2.2.3. Conversion of the fatty acyl ether chloride to NGAS



In a round bottom flask, glucosamine hydrochloride (4.3 g, 20 mmol) was added to 4. Next, triethylamine (5.5 mL, 40 mmol) was added to the reaction content and the resulting mixture was stirred for 4-5 hours at ambient temperature. The completion of the reaction was monitored by TLC, using ethyl acetate/petroleum ether (1:1) as the eluent. NGAS 6 (mp 200-202 °C) was obtained in 75% yield (5.2 g).

### 2.3. Surface properties calculations

The surface parameters,  $\Gamma_{\max}$  (the maximum surface excess concentration),  $A_{\min}$  (minimum surface area per surfactant molecule), pC20 (adsorption efficiency), P (packing parameter),  $\Delta G^{\circ}_{\text{mic}}$  (free energy of micellization),  $\Delta G^{\circ}_{\text{ads}}$  (free energy of adsorption), and HLB (hydrophilic-lipophilic balance) were calculated using the equations 1-7, respectively [6, 27].

$$\Gamma_{\max} = -\frac{1}{2.303RTn} \left( \frac{\partial \gamma}{\partial \log C} \right) \quad (1)$$

$$A_{\min} = 10^{20} / N_A \cdot \Gamma \quad (2)$$

$$pC20 = -\log C20 \quad (3)$$

$$P = (V_H / I_c a_0) \quad (4)$$

$$\Delta G^{\circ}_{\text{mic}} = RT \ln X_{\text{cmc}} \quad (5)$$

$$\Delta G^{\circ}_{\text{ads}} = \Delta G^{\circ}_{\text{mic}} - \left( \frac{\pi_{\text{cmc}}}{\Gamma_{\max}} \right) \quad (6)$$

$$HLB = \frac{20G}{G+A} \quad (7)$$

## 3. Results and Discussion

### 3.1. Characterization of NGAS

The product was characterized using various analytical techniques including MS spectroscopy and FT-IR. The mass spectrum of NGAS showed a molecular ion peak ( $M^+$ ) at  $m/z$  405, corresponding to the molecular weight of the surfactant (Fig. 2, top). Major fragmentation peaks observed in the

mass spectrum are summarized in Table 1. The FTIR spectrum of NGAS showed characteristic peaks corresponding to the functional groups present in the molecule (Fig. 2, middle). The broad peak at  $3460 \text{ cm}^{-1}$  was attributed to O-H stretching vibrations, while the peak at  $3295 \text{ cm}^{-1}$  was attributed to the N-H stretching vibrations of the amide group. In addition, the peak at  $1600 \text{ cm}^{-1}$  was assigned to the C=O stretching vibrations of the amide group. Additionally, the peaks at  $1105 \text{ cm}^{-1}$  was assigned to C-O-C stretching vibrations, indicating the presence of ether linkages in the molecule. To further support the structural elucidation, superimposition of the IR spectra of NGAS and its precursor is presented in Fig. 2, bottom.

**Table 1.** Major mass spectrum fragmentation peaks of NGAS

| $m/z$ | Relative intensity % | $m/z$ | Relative intensity % |
|-------|----------------------|-------|----------------------|
| 404   | 0.1                  | 142   | 2.0                  |
| 368   | 3.0                  | 111   | 22.0                 |
| 242   | 0.5                  | 96    | 42.0                 |
| 220   | 1.0                  | 83    | 56.0                 |
| 202   | 32                   | 52    | 100                  |

### 3.2. Surface tension measurements

The surface tension measurements for dilute aqueous solutions of NGAS, performed at 298.15 K, are provided in Table 2. The surface tension data of C12GA were collected from the literature [36]. The corresponding surface tension curve of aqueous solutions of NGAS has been shown in Fig. 3. At first, the surface tension decreases with increasing the concentration of the component, indicating that the surfactant molecule is adsorbed in the interface. Then, a plateau region with an almost constant slope appears in the  $(\gamma - \log[C])$  plot, indicating that a stable micelle has been created. The minimum surface tension ( $\gamma_{\text{CMC}}$ ) value is obtained by the analysis of the plateau region of the plots. The critical micelle concentration (CMC) is determined at the intersection of the two fitting straight lines

above and below the breaking point of the tension vs (log) concentration plot using a linear regression

analysis method. A summary of the data is compiled in Table 3.

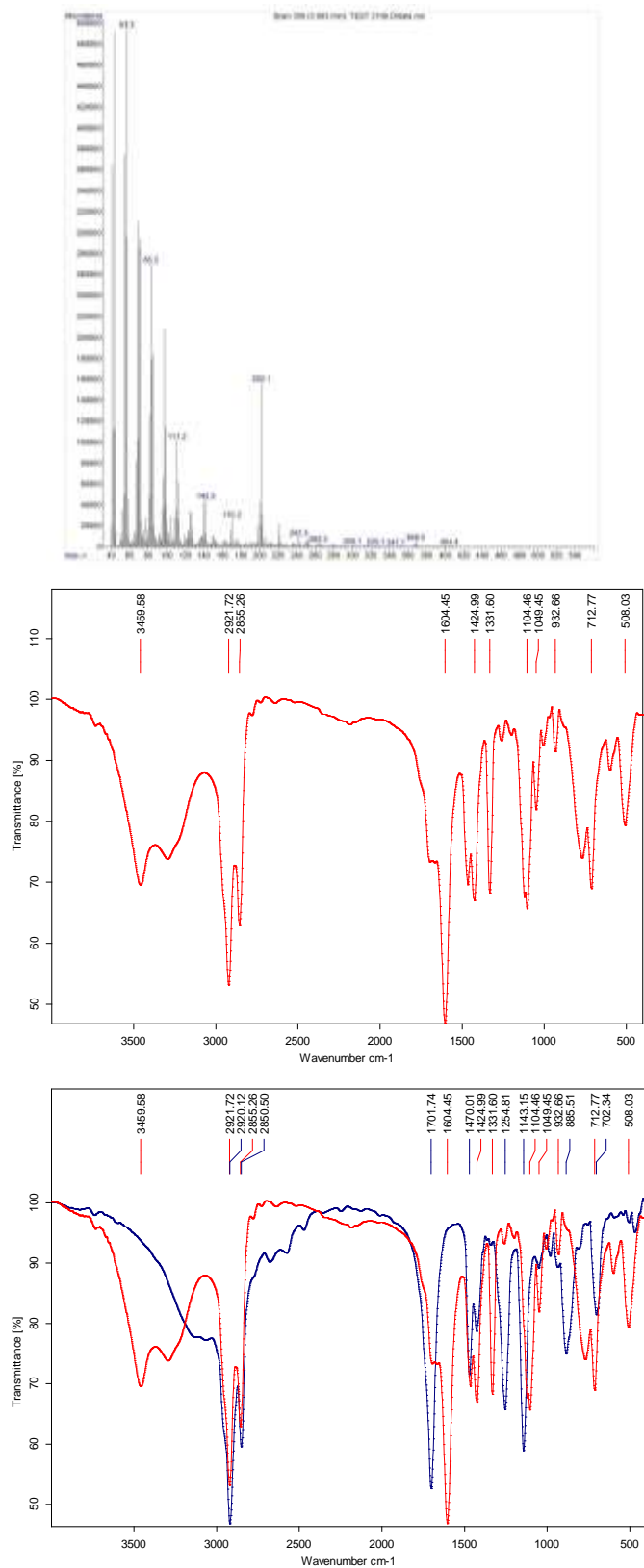
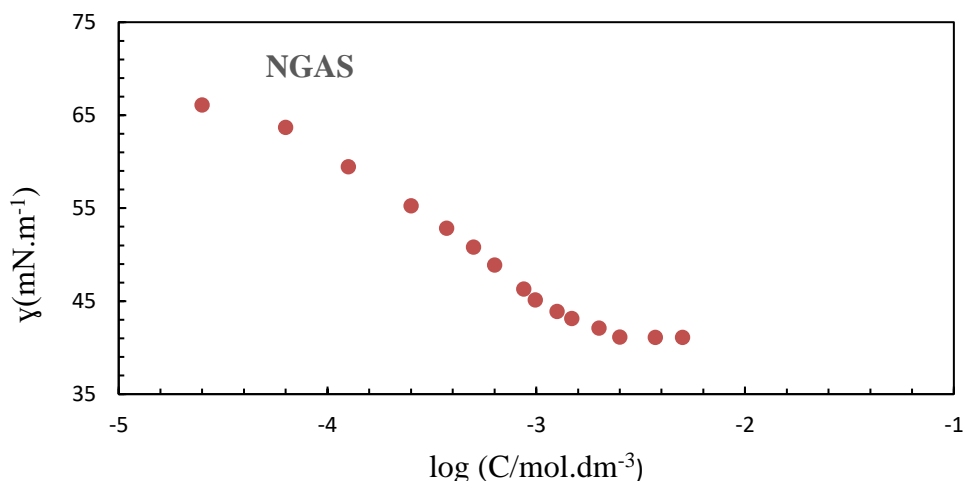


Fig. 2. (top) MS spectrum, (middle) FT-IR spectrum, and superimposition of the IR spectra of NGAS (red) and its precursor (blue) (bottom).

**Table 2.** Surface tension of NGAS in aqueous media at different concentrations at 298.15 K

| Entry | g/l   | ppm  | C(M)     | log (c/mol.dm <sup>-3</sup> ) | $\gamma$ mN.m <sup>-1</sup> |
|-------|-------|------|----------|-------------------------------|-----------------------------|
| 1     | 0     | 0    | 0        |                               | 72.1                        |
| 2     | 0.01  | 10   | 2.47E-05 | -4.6                          | 66.1                        |
| 3     | 0.025 | 25   | 6.17E-05 | -4.2                          | 63.69                       |
| 4     | 0.05  | 50   | 1.23E-04 | -3.9                          | 59.47                       |
| 5     | 0.1   | 100  | 2.47E-04 | -3.6                          | 55.25                       |
| 6     | 0.15  | 150  | 3.70E-04 | -3.43                         | 52.86                       |
| 7     | 0.2   | 200  | 4.94E-04 | -3.3                          | 50.8                        |
| 8     | 0.25  | 250  | 6.17E-04 | -3.2                          | 48.9                        |
| 9     | 0.35  | 350  | 8.64E-04 | -3.06                         | 46.3                        |
| 10    | 0.4   | 400  | 9.88E-04 | -3.005                        | 45.12                       |
| 11    | 0.55  | 550  | 1.36E-03 | -2.9                          | 43.9                        |
| 12    | 0.6   | 600  | 1.48E-03 | -2.83                         | 43.15                       |
| 13    | 0.8   | 800  | 1.98E-03 | -2.7                          | 42.1                        |
| 14    | 1     | 1000 | 2.47E-03 | -2.6                          | 41.15                       |
| 15    | 1.5   | 1500 | 3.70E-03 | -2.43                         | 41.1                        |
| 16    | 2     | 2000 | 4.94E-03 | -2.3                          | 41.1                        |

**Fig. 3.** Plot of equilibrium surface tension of aqueous solutions of NGAS versus log C.**Table 3.** Micellar and surface properties of NGAS & C12GA

| Compound                                    | NGAS                  | G <sub>12</sub> GA [36] |
|---|-----------------------|-------------------------|
| CMC (mol.L <sup>-1</sup> )                  | $2.06 \times 10^{-3}$ | $7.76 \times 10^{-5}$   |
| $\gamma_{CMC}$ (mN.m <sup>-1</sup> )        | 41.90                 | 28.4                    |
| $\Gamma_{max}$ (mol. m <sup>-2</sup> )      | 2.65                  | 4.60                    |
| pC <sub>20</sub>                            | 3.43                  | 5.02                    |
| A <sub>min</sub> (Å <sup>2</sup> /molecule) | 62.55                 | 36.1                    |
| $\Delta G_{ads}^{\circ}$ (kJ/mol)           | -36.68                | -42.8                   |
| $\Delta G_{mic}^{\circ}$ (kJ/mol)           | -25.29                | -33.6                   |

Comparison of CMC values of NGAS with those of C12GA suggests that NGAS has a larger CMC than C12GA does. This could be due to having additional ether and NH functional groups residing in the NGAS structure, making NGAS more polar than C12GA. This may result in lower tendency in migration of molecules from the bulk solution to the

interface and higher concentrations formation of micelles.

The surface excess concentrations ( $\Gamma_{max}$ ) in mol/m<sup>2</sup>, and minimal area/molecule ( $A_{min}$ ) in Å<sup>2</sup>, at the interface of water and air were calculated from Eq. (1) and Eq. (2) [37-39], where  $(\frac{\partial \gamma}{\partial \log c})$  is the slope below the CMC in the surface tension plot, T is the temperature (K), R = 8.314 (J/mol K), n is 1 for

nonionic surfactants, and  $N_A$  = Avogadro constant. Another important parameter is pC20, which is calculated as shown in Eq. (3) [40], Where pC<sub>20</sub> is the efficiency of surface adsorption, and the negative log of the bulk surfactant concentration, C<sub>20</sub>, required to reduce the surface tension of the solvent by 20 mN/m.

Comparison of  $\Gamma_{\max}$  and  $A_{\min}$  values of NGAS with those of C12GA (shown in Table 3) suggests that NGAS has lower  $\Gamma_{\max}$  and larger  $A_{\min}$  than C12GA does. This is due to the special structure of the ring head of NGAS. Increased charge repulsion in the ring structure of NGAS compared to the linear structure of C12GA (with similar alkyl chain lengths, (C<sub>12</sub>H<sub>25</sub>), leads to a lower packing density at the air-water interface and subsequently to an increase in the  $A_{\min}$  value of the NGAS molecule. Moreover, the value of pC20 for NGAS is lower than that of C12GA, which indicates the low tendency of NGAS to be absorbed at the interface compared to the tendency to enter the bulk. Also, the results of Table 3 show that the values of  $\gamma_{\text{CMC}}$  for NGAS is greater than those of C12GA and this surface activity is due to the decreased solubility of NGAS in the oil phase and low tendency to migrate from the bulk to the interface.

The packing parameter (P) is calculated as shown in Eq. (4), where P determines the shape of the micelle, ( $V_H$ ) is the volume occupied by the hydrophobic groups in the micellar core,  $l_c$  is the length of the hydrophobic group in the core, and  $a_0$  is the cross-sectional area occupied by the hydrophilic group at the micelle–solution interface. According to the packing parameter value of NGAS ( $P < 1/3$ ), the structure of its micelle is spheroidal in aqueous media.

The standard free energy of micellization per mole of the monomer unit ( $\Delta G^{\circ}_{\text{mic}}$ ) of the surfactant is related to the CMC, as shown by Eq. (5) [41], where  $X_{\text{CMC}}$  is the CMC as a molar fraction (CMC/55.5).

The free energy of adsorption  $\Delta G^{\circ}_{\text{ad}}$  at the air/water interface is calculated from the Eq. (6) [42], where ( $\Pi_{\text{cmc}}$ ) is the surface pressure at CMC. The free energy of micellization ( $\Delta G^{\circ}_{\text{mic}}$ ) (Eq. 5) and adsorption ( $\Delta G^{\circ}_{\text{ads}}$ ) (Eq. 6) of the glucosamide surfactants (NGAS and C12GA) are a negative value, indicating that the processes are desired thermodynamically. The magnitude of  $\Delta G^{\circ}_{\text{ads}}$  is more negative than that of  $\Delta G^{\circ}_{\text{mic}}$ , signifying that the adsorption process is more favorable than micellization. The values of  $\Delta G^{\circ}_{\text{mic}}$  and  $\Delta G^{\circ}_{\text{ads}}$  are collected in Table 3.

### 3.3. Hydrophilic and hydrophobic balance parameter (HLB)

HLB criterion helps to choose the suitable surfactant so that surfactants with low HLB of 2-3 are suitable as antifoam, while those with HLB of 3-6 can be used as emulsifier for water-in-oil (W/O) emulsion systems. In addition, surfactants with HLB of 7-9 are useful as wetting agents, and those with HLB of 8-16 are suitable for oil-in-water (O/W) emulsions. Finally, surfactants with HLB above 13 can be used as cleaners and resolving agents [43]. The HLB values of the two non-ionic surfactants NGAS and C12GA were determined according to Griffin's Eq. (7) [44], where A is the molecular mass of the whole molecule, and G is the molecular mass of the hydrophilic part of the molecule.

The value of the HLB for NGAS with a molecular weight of 405 gmol<sup>-1</sup> determined to be equal to 11.65, while it was found to be equal to 11.35 for C12GA with a molecular weight of 391 gmol<sup>-1</sup>. According to these HLB values, both surfactants can be used as emulsifiers in the oil-water system.

### 4. Conclusions

In summary, surface behaviours and micellization of the two nonionic surfactants, NGAS and C12GA, with similar alkyl chain lengths, were investigated for the first time by the tensiometric method, and the following results were concluded:

1. comparison of CMC between the two surfactants shows that the CMC value is higher for NGAS, due to more excellent solubility in the aqueous phase,
2. the obtained results indicate that  $\Gamma_{\max}$  decreased and  $A_{\min}$  increased with increasing hydrophilicity,
3. surfactant adsorption efficiency in water-air interface ( $pC_{20}$ ) decreases with increasing hydrophilicity,
4. the negative values of  $\Delta G^{\circ}_{\text{mic}}$  and  $\Delta G^{\circ}_{\text{ads}}$  in both of the surfactants show that surfactant adsorption and micelle formation at the interface are spontaneous processes,
- 5- moreover, it was found that the adsorption of the surfactant at the air-water interface is more favourable than the micelle formation (or  $|\Delta G^{\circ}_{\text{mic}}| < |\Delta G^{\circ}_{\text{ads}}|$ ), and
6. HLB measurements show that both NGAS and C12GA with HLB values equal to 11.65 and 11.35 can be used as emulsifiers for the O/W systems.

#### Acknowledgments

The authors gratefully appreciate Department of Chemistry and especially Research Department of Islamic Azad University of Arak for their kind financial supports.

#### Conflicts of Interest

The author declares that there is no conflict of interest regarding the publication of this manuscript.

#### References

- [1] Kandasamy, R., Rajasekaran, M., Venkatesan, S. K., & Uddin, M. (2019). *New trends in the biomanufacturing of green surfactants: biobased surfactants and biosurfactants*. American Chemical Society.
- [2] Taheri, E., & Bagheri, A. (2018). Analysis of surface and micellar phases in binary mixture of surfactant and ionic liquid by surface tension measurement. *Applied Chemistry Today*, 13(48), 167-180.

- [3] Abdous, B., Sajjadi, S.M., & Bagheri, A. (2022). Determining the aggregation number of anionic surfactants based on conductivity method: employing QSAR-ANN modelling techniques for predicting the aggregation number of surfactants. *Applied Chemistry Today*, 17(63), 87-108.
- [4] Bagheri, A. (2021). Interfacial micellization properties of pure surfactants with similar hydrocarbon chain length ( $C_{16}H_{33}$ ) and different polar head in aqueous medium. *Applied Chemistry Today*, 15(57), 55-64.
- [5] Rajabi, M., Arab, A., & Bagheri, A. (2021). The inhibition effect of CTAB and Triton X-100 surfactants on the corrosion of nickel in alkaline solution. *Applied Chemistry Today*, 16(59), 63-72.
- [6] Rosen, M. J.; Kunjappu, J. T. (2012). *Surfactants and interfacial phenomena*, 4th Ed., John Wiley & Sons, Inc., New York USA.
- [7] Maleki, S., Mennati, A., & Salehi Sadaghiani, A. R. (2011). Determine and compare the cmc point of SDS, Triton x-100 and CTAB surfactants using conductometry method. *Applied Chemistry Today*, 6(20), 47-52.
- [8] Bagheri, A., & Rafati, A. A. (2014). Thermodynamic investigation of inclusion complex formation between cetyltrimethyl ammonium bromide (CTAB) and  $\beta$ -cyclodextrin at various temperatures. *Journal of Molecular Liquids*, 195, 145-149.
- [9] Kovensky J., & Grand E. (2016). *Recent advances in the synthesis of sugar-based surfactants*. RSC Green Chemistry, London UK, p. 159-204.



- [10] Bazito, R. C., & El Seoud, O. A. (2002). Sugar-based surfactants: adsorption and micelle formation of sodium methyl 2-acrylamido-2-deoxy-6-*O*-sulfo-*D*-glucopyranosides. *Langmuir*, 18(11), 4362-4366.
- [11] Teng, Y., Stewart, S. G., Hai, Y. W., Li, X., Banwell, M. G., & Lan, P. (2020). Sucrose fatty acid esters: synthesis, emulsifying capacities, biological activities and structure-property profiles. *Critical Reviews in Food Science and Nutrition*, 61(19), 3297-3317.
- [12] Maugard, T., Remaud-Simeon, M., Petre, D., & Monsan, P. (1997). Lipase-catalysed synthesis of biosurfactants by transacylation of *N*-methyl-glucamine and fatty-acid methyl esters. *Tetrahedron*, 53(22), 7629-7634.
- [13] Cristobal, C. R. (2008). *Sugar-based surfactants: fundamentals and applications*. Marcel Dekker: New York.
- [14] Holmberg, K. (2003). *Novel surfactants: preparation, applications, and biodegradability*. 2nd edn. Marcel Dekker: New York.
- [15] Plat, T., & Linhardt, R. (2001). Syntheses and applications of sucrose-based esters. *Journal of Surfactants and Detergents*, 4(4), 415-421.
- [16] Satge, C., Granet, R., Verneuil, B., Champavier, Y., & Krausz, P. (2004). Synthesis and properties of new bolaform and macrocyclic galactose-based surfactants obtained by olefin metathesis. *Carbohydrate Research*, 339(7), 1243-1254.
- [17] Hill, K., & Rhode, O. (1999). Sugar-based surfactants for consumer products and technical applications. *Lipid – Fett*, 101(1), 25-33.
- [18] Zhi, L., Li, J., Li, X., Chen, Y., Song, Y., Yu, J., & Zhang, Q. (2019). Enhancing water solubility of *N*-dodecyl-*D*-gluconamide surfactant using borax. *Chemical Physics Letters*, 725, 87-91.
- [19] Kida, T., Yurugi, K., Masuyama, A., Nakatsuji, Y., Ono, D., & Takeda, T. (1995). Preparation and properties of new surfactants containing *D*-glucosamine as the building block. *Journal of the American Oil Chemists Society*, 72(7), 773-780.
- [20] Burczyk, B., Wilk, K. A., Sokolowski, A., & Syper, L. (2001). Synthesis and surface properties of *N*-alkyl-*N*-methylgluconamides and *N*-alkyl-*N*-methyl lactobionamides. *Journal of Colloid and Interface Science*, 240(2), 552-558.
- [21] Laughlin, R. G., Fu, Y.-C., Wireko, F. C., Scheibel, J. J., & Munyon, R. L. (2003). **N*-Alkanoyl-*N*-alkyl-1-glycamines in: novel surfactants: preparation, applications, and biodegradability*. Marcel Dekker: New York.
- [22] Han, F., & Zhang, G. (2004). New family of gemini surfactants with glucosamide-based trisiloxane. *Colloids and Surfaces A: Physicochemical and Engineering Aspects*, 237(1-3), 79-85.
- [23] Han, F., & Zhang, G. Synthesis and characterization of glucosamide-based trisiloxane gemini surfactants. (2004). *Journal of Surfactants and Detergents*, 7(2), 175-180.
- [24] Gaber, Y., Tornvall, U., Orellana-Coca, C., Amin, M. A., & Hatti-Kaul, R. (2010). Enzymatic synthesis of *N*-alkanoyl-*N*-methylglucamide surfactants: solvent-free production and environmental assessment. *Green Chemistry*, 12(10), 1817-1825.

- [25] Han, F., Deng, Y., Wang, P., Song, J., Zhou, Y., & Xu, B. (2012). Synthesis and characterization of glucosamide surfactant. *Journal of Surfactants and Detergents*, 16(2), 155-159.
- [26] Zhang, H., Lu, Y., Wang, Y., Zhang, X., & Wang, T. (2018). D-Glucosamine production from chitosan hydrolyzation over a glucose-derived solid acid catalyst. *RSC Advances*, 8(10), 5608-5613.
- [27] Ji, S., Shen, W., Chen, L., Zhang, Y., Wu, X., Fan, Y., Fu, F., & Chen, G. (2019). Synthesis and properties of sugar-based surfactants alkoxyethyl  $\beta$ -D-glucopyranoside. *Colloids and Surfaces A: Physicochemical and Engineering Aspects*, 564, 59-68.
- [28] Michocka, K., Staszak, K., Gwiazdowska, D., & Wiczorek, D. (2019). Synthesis, surface and antimicrobial activity of new lactose-based surfactants. *Molecules*, 24(21), 4010-4023.
- [29] Haghghi, O. M., Zargar, G., Manshad, A. K., Ali, M., Takassi, M. A., Ali, J. A., & Keshavarz, A. (2020). Effect of environment-friendly non-ionic surfactant on interfacial tension reduction and wettability alteration; implications for enhanced oil recovery. *Energies*, 13(15), 3988-4004.
- [30] Wang, L., & Queneau, Y. (2019). *Carbohydrate-based amphiphiles: resource for bio-based surfactants*. Green Chemistry and Chemical Engineering; Springer: p. 349-383.
- [31] Moldes, A. B., Rodríguez-López, L., Rincón-Fontán, M., López-Prieto, A., Vecino, X., & Cruz, J. M. (2021). Synthetic and bio-derived surfactants versus microbial biosurfactants in the cosmetic industry: an overview. *International Journal of Molecular Sciences*, 22(5), 2371-2393.
- [32] Lubberink, M., Finnigan, W., Schnepel, C., Baldwin, C. R., Turner, N. J., & Flitsch, S. L. (2022). One-step biocatalytic synthesis of sustainable surfactants by selective amide bond formation. *Angewandte Chemie International Edition*, 61(30), e202205054.
- [33] Rastegar Fatemi, S. E., Shafiei, H., & Mojtahedi, M. M. (2023). Theoretical and experimental investigation of eco-friendly nonionic surfactant based on glucosamine and extraction of relevant constants. *Letters in Organic Chemistry*, 2(21), 163-191.
- [34] Jaeun, K., Jaemin, L., Hyuk, D., Hyun, D. S., Kwon, K. S., & Jung, P. S. (2023). Acid addition salts of indene derivative prodrug and its preparation methods. US2023399298A1.
- [35] Hato, M., Shinoda, K., & Miyagawa, T. (1976). Physico-chemical properties of aqueous solutions of  $C_{n-1}H_{2n-1}OCH_2CO_2Na$ . *Bulletin of the Chemical Society of Japan*, 49(5), 1257-1259.
- [36] Zhu, Y. P., Rosen, M. J., Vinson, P. K., & Morral, S. W. (1999). Surface properties of *N*-alkanoyl-*N*-methylglucamines and related materials. *Journal of Surfactants and Detergents*, 2, 357-362.
- [37] Gao, S., Song, Z., Zhu, D., Lan, F., & Jiang, Q. (2018). Synthesis, surface activities, and aggregation behavior of phenyl-containing carboxybetaine Surfactants. *RSC Advances*, 8(58), 33256-33268.
- [38] Abdel-Raouf, M. E.-S., Abdul-Raheim, A.-R. M., & Abdel-Azim, A.-A. A. (2011). Surface properties and thermodynamic parameters of some sugar-based ethoxylated

aminesurfactants: 1-synthesis, characterization, and demulsification efficiency. *Journal of Surfactants and Detergents*, 14(1), 113-121.

[39] Sameer, H. K., & Bahar, S. (2015). Adsorption properties for aqueous solution of binary mixture of cocamidopropyl betaine-sodiumdodecyl sulfate surfactants on air-liquid interface. *International Journal of Sciences: Basic and Applied Research*, 24(3), 50-58.

[40] Wang, L., Zhang, Y., Ding, L.; Liu, J., Zhao, B.; Deng, Q., & Yan, T. (2015). Synthesis and physiochemical properties of novel gemini surfactants with phenyl-1,4-bis(carbamoylmethyl) Spacer. *RSC Advances*, 5(91), 74764-74773.

[41] Vafakish, B., & Wilson, L. D. (2021). A review on recent progress of glycan-based

surfactant micelles as nanoreactor systems for chemical synthesis applications. *Polysaccharides*, 2(1), 168-186.

[42] Shah, S. K., & Bhattarai, A. (2020). Interfacial and micellization behavior of cetyltrimethylammonium bromide (CTAB) in water and methanol-water mixture at 298.15 to 323.15 K. *Journal of Chemistry*, 2020, 1-13.

[43] Rokhati, N., Kusworo, T. D., Prasetyaningrum, A., Hamada, N. A., Utomo, D. P., & Riyanto, T. (2022). Effect of surfactant HLB value on enzymatic hydrolysis of chitosan. *Chemical Engineering*, 6(1), 17-28.

[44] Griffin, W. C. (1954). Calculation of HLB values of non-ionic surfactants. *Journal of the Society of Cosmetic Chemists*, 5(4), 249-256.

